encit 2020

ABCM Associação Brasileira de Engenharia e Ciências Mecânicas

18th Brazilian Congress of Thermal Sciences and Engineering
November 16-20, 2020 (Online)

ENC-2020-0649
PRELIMINARY DESIGN AND ANALYSIS OF A GENERIC SCRAMJET AIR FOR ATMOSPHERIC FLIGHT AT MACH NUMBER 5.8

José Fernandes Filho
Lucas de Almeida Sabino Carvalho
Luísa Mirelle Costa dos Santos
George Santos Marinho
Universidade Federal do Rio Grande do Norte/UFRN - Centro de Tecnologia. Av. Senador Salgado Filho, 3000 - Campus Universitário, Lagoa NovaCEP 59.078-970 – Natal/RN- Brasil
josef1703@hotmail.com, carvalholucas01@hotmail.com, luisasantos98@hotmail.com, gmarinho@ct.ufrn.br.

José Bismark de Medeiros
Universidade Federal do Vale do São Francisco/UNIVASF –Colegiado Acadêmico de Engenharia Mecânica. Campus Juazeiro. Av.Antonio Carlos Magalhães, 510–Santo Antonio. CEP 48.902-300 - Juazeiro, BA- Brasil
jose.bismark@univasf.edu.br

Paulo Gilberto de Paula Toro
Universidade Federal do Rio Grande do Norte/UFRN - Centro de Tecnologia. Av. Senador Salgado Filho, 3000 - Campus Universitário, Lagoa NovaCEP 59.078-970 – Natal/RN- Brasil
Toro11pt@gmail.com

Abstract. *The calculations for this project are based on the following parameters: A one-dimensional (1–D) theoretical analysis was applied to design a generic scramjet flying at Mach number 5.8 and 20 km of geometric altitude, to demonstrate the supersonic combustion of air/hydrogen mixture; Plane oblique shockwave theory (1–D flow), with heat addition (Raleigh flow) theory, and expansion wave (Prandtl-Meyer) theory coupled to the area ratio theory are applied to the compression, combustion chamber and expansion sections, respectively; The scramjet inlet is compound by three ramps with the following deflection angles: 7.25º, 8.6º and 10.3º. The Mach number of 1.1 is assumed to avoid the shocked flow at the exit of the combustion chamber; To expand the combustion products is assumed the expansion deflection angles of 10º and 15º at the expansion section. Based on the results, data variations will be displayed and whether or not thrust was generated.*

Keywords: *scramjet, supersonic combustion ramjet, hypersonic airbreathing propulsion*

1. INTRODUCTION

The current scenario in the aerospace sector, there are several countries developing vehicles to fly at hypersonic speeds, which uses scramjet engines (supersonic combustion ramjet), a technology that combines the advantages of low weight and high specific impulse when comparing with the conventional rocket engines (**Fry, 2004**).

Some research centers have already been successful in developing experimental flight test demonstrators, for example, the X-51, developed by DARPA – Defense Advanced Research Projects Agency (**Hank et al., 2008**). In addition, the Centre for Hypersonics (The University of Queensland, Australia) developed the HyShot (**Paull et al., 2006**) and the NASA and AFRL (Australia's Defence Science and Technology Organisation) are working on the HIFiRE project (**Dolvin, 2008**). The Hexafly International project is a consortium project in developing by European Union Partners (**Steelant et al., 2018**).

The Instituto de Estudos Avançados (IEAv / Brazil) is developing the scramjet 14-X S project, to demonstrate the supersonic combustion at a geometric altitude of 30 km, at Mach number 7 (**Costa et al., 2016**).

In the present work, developed in the Postgraduate Program in Aerospace Engineering (Federal University of Rio Grande do Norte - Brazil), an aerospace technological vehicle was designed to demonstrate the supersonic combustion, during the atmosphere flight at Mach number 5.8 at a geometric altitude of 20 km.

2. METHODOLOGY

The procedures for carrying out the analytical study were divided into four parts:

2.1 Scramjet characteristics

According with **Heiser and Pratt (1994)** the scramjet may be divided in three main components and by several stations (**Fig. 1**): external (stations 0 to 1), and internal (stations 1 to 3) compression section (inlet, governing by oblique shockwave theory), combustor (stations 3 to 4, governing by 1–D flow with heat addition, Rayleigh flow theory) and internal (stations 4 to 9) and external (stations 9 to 10) expansion section (outlet, governing by expansion wave, Prandtl-Meyer theory and area ratio).

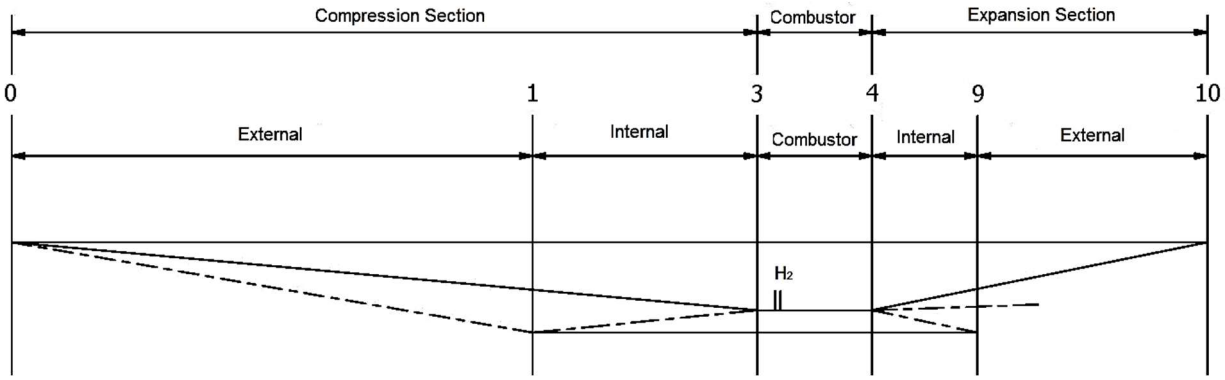

Figure 1: Airframe-integrated scramjet engine stations and reference terminology to a hypersonic vehicle (adapted from Heiser and Pratt, 1994).

An important feature of the scramjet is its highly integrated system, where propulsion system and vehicle are indistinguishable. This tight integration is caused by the fact that the front section of the vehicle contributes to the compression of atmospheric air, while the rear section contributes to the generation of thrust. The net thrust produced by the scramjet is the difference between the thrust (force that propels the vehicle) generated by the expansion of exhaust gases from the rear section of the engine and the total drag (force that resists to the vehicle movement).

Finally, the incident shock wave (dashed line in **Fig. 1**), from the external compression section, reaches the leading-edge of the cowl (shock on-lip), and the reflected shock wave, in the internal compression section, reaches the entrance of the combustion chamber (shock on-corner). Therefore, the air capture area should be maximum and the length of the scramjet compression section should be minimum. The subscripts *in* and *out* are used to identify the upstream (inlet) and the downstream (outlet) conditions, respectively, of each station of any scramjet design.

2.2 Governing equations

Analytical theoretical analysis may be used to calculate the thermodynamic properties (pressure, temperature, density, sound velocity and Mach number) at the flow path from the leading-edge to the trailing-edge of the hypersonic vehicle with airframe-integrated scramjet. The analysis provides closed form relationships to determine the thermodynamic air property ratios and Mach number applied to one-dimensional compressible flow (shock wave) theory, one-dimensional flow with heat addition and the one-dimensional compressible flow (expansion wave) theory coupled to area ratio. This approach is used to design the compression, combustor and expansion sections, of any scramjet.

Oblique shock wave relationships

Considering no boundary-layer effects (non-viscous flow) and calorically perfect gas ($p = \rho RT$, $\gamma = \text{constant}$), the incident oblique shock wave relationships, applied at the leading-edge of the aerospace vehicle, as well as at the intersection of two consecutively plane surfaces and at reflected oblique shock wave, can be easily obtained as closed form of the shock wave angle β, the thermodynamic (static pressure, static density, static temperature, sound velocity) property ratios and Mach number across the oblique shock as function of the incoming local supersonic/hypersonic flow Mach number M_{in}, the gas from the atmosphere γ (air in the Earth's planet, $\gamma = 1.4$) and the deflection angle θ (Anderson, 1990). **Figure 2** shows the incident and reflected shock waves.

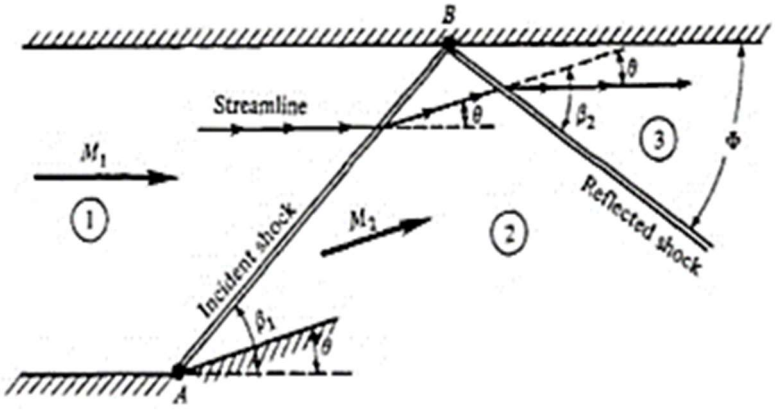

Figure 2. Incident and reflected oblique shockwaves (Anderson, 1990).

The shock wave angle β (**Fig. 2**), the Mach number after the shock wave and the thermodynamic property ratios are given by:

$$tg\theta = 2(\text{cotg}\,\beta)\left[\frac{\left(M_{in}\ sen\beta\right)^2 - 1}{M_{in}^2(\gamma + \cos 2\beta) + 2}\right] \tag{1}$$

$$M_{out} = \frac{\sqrt{\dfrac{\left(M_{in}\ sen\beta\right)^2 + \dfrac{2}{(\gamma-1)}}{\dfrac{2\gamma}{(\gamma-1)}\left(M_{in}\ sen\beta\right)^2 - 1}}}{sen\left(\beta - \theta_s\right)} \tag{2}$$

$$\frac{p_{out}}{p_{in}} = 1 + \frac{2\gamma}{(\gamma+1)}\left[\left(M_{in}\ sen\beta\right)^2 - 1\right] \tag{3}$$

$$\frac{\rho_{out}}{\rho_{in}} = \frac{\left[(\gamma+1)\left(M_{in}\ sen\beta\right)^2\right]}{\left[(\gamma-1)\left(M_{in}\ sen\beta\right)^2 + 2\right]} \tag{4}$$

$$\frac{T_{out}}{T_{in}} = \frac{\dfrac{p_{out}}{p_{in}}}{\dfrac{\rho_{out}}{\rho_{in}}} = \left\{1 + \frac{2\gamma}{(\gamma+1)}\left[\left(M_{in}\ sen\beta\right)^2 - 1\right]\right\}\left\{\frac{\left[(\gamma-1)\left(M_{in}\ sen\beta\right)^2 + 2\right]}{\left[(\gamma+1)\left(M_{in}\ sen\beta\right)^2\right]}\right\} \tag{5}$$

It is important point out that the plane oblique shock wave theory may be used to determine the flow conditions after the incident shock wave established (attached) at the leading-edge with the turning angle θ_1. The same theory may be used not only to the incident shock wave established (attached) at the intersection of two compression surfaces with the turning angle θ_2, but also to the reflected shock wave with the turning angle θ_3. The flow after the reflected shock wave should be aligned to the confined structure (**Fig. 2**).

The thermodynamic property ratios may be obtained in any gas dynamic textbooks – e. g., **Anderson (1990)**. The flow across the plane oblique shock wave promotes an increase of pressure, density, temperature, and a decrease of Mach number. However, the flow remains supersonic/hypersonic and parallel to the flat surface of the compression section of the vehicle with airframe-integrated scramjet engine lower surface (**Fig. 2**).

<u>One-dimensional flow with heat addition</u>

The combustion processes correspond to heat addition at constants pressure, density, temperature and Mach number at the inlet of the scramjet combustor (**Fig. 3**).

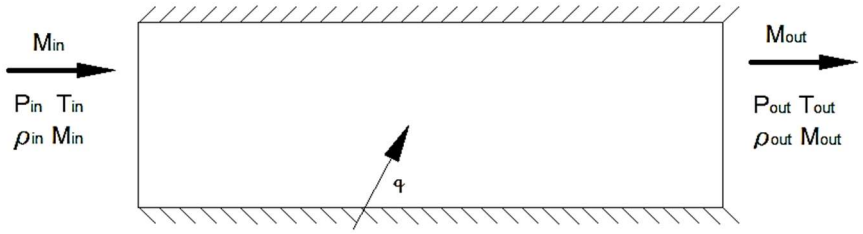

Figure 3. Rayleigh Flow, one-dimensional with constant-area heat addition.

The heat addition to 1-D, constant-area, Rayleigh flow analysis, may be applied to the combustion processes between the entrance and the exit of the scramjet combustor.

The conditions at the entrance of the combustion chamber are given by the thermodynamic properties and Mach number estimated just right after the reflected shock wave at the internal compression section.

For the calorically perfect gas ($p = \rho RT$, $\gamma = \text{constant}$), and considering no boundary-layer effects, the analytical relationships are easily obtained as a function of the Mach number (M_{in}) of the local supersonic inlet flow, and the properties of the gas from the atmosphere ($\gamma = 1.4$) (**Anderson, 1990**).

The heat added to the flow due to the change in total energy (temperature), is given by:

$$q = \dot{m}_0 \; c_p \left(T_{o,out} - T_{o,in} \right) \tag{6}$$

where the captured air mass flow rate and total temperature are given by:

$$\frac{T_o}{T} = 1 + \frac{\gamma - 1}{2} M^2 \tag{7}$$

$$\dot{m}_0 = \rho_0 u_0 A_0 \tag{8}$$

Closed-form of the thermodynamic property (static pressure, static density, static temperature and total temperature) ratios across constant-area heat addition are given by:

$$\frac{p_{out}}{p_{in}} = \left(\frac{1 + \gamma M_{in}^2}{1 + \gamma M_{out}^2} \right) \tag{9}$$

$$\frac{\rho_{out}}{\rho_{in}} = \left(\frac{1 + \gamma M_{out}^2}{1 + \gamma M_{in}^2} \right) \left(\frac{M_{in}}{M_{out}} \right)^2 \tag{10}$$

$$\frac{T_{out}}{T_{in}} = \frac{\dfrac{p_{out}}{p_{in}}}{\dfrac{\rho_{out}}{\rho_{in}}} = \left(\frac{1 + \gamma M_{in}^2}{1 + \gamma M_{out}^2} \right)^2 \left(\frac{M_{out}}{M_{in}} \right)^2 \tag{11}$$

$$\frac{T_{o,out}}{T_{o,in}} = \left(\frac{1 + \gamma M_{in}^2}{1 + \gamma M_{out}^2} \right)^2 \left(\frac{M_{out}^2}{M_{in}^2} \right)^2 \left(\frac{1 + \frac{\gamma - 1}{2} M_{out}^2}{1 + \frac{\gamma - 1}{2} M_{in}^2} \right) \tag{12}$$

The Rayleigh flow (1-D flow with heat addition) may be applied to the combustion process to burn H_2 and O_2 in supersonic speed, resulting in an increase of static pressure, static density, static temperature at the exit of the combustor chamber (outlet) and in a decrease of the Mach number of the combustion product flow.

Burn hydrogen with supersonic airflow

The chemical energy rate available to the scramjet engine is given by (**Heiser e Pratt, 1994**):

$$\text{chemical energy rate} = \dot{m}_{\text{fuel}}\ h_{pr} \tag{13}$$

where: h_{pr} is the heat of reaction – for hydrogen it is 119,954 J/kg (**Heiser and Pratt, 1994**). The chemical energy rate should be the heat addition estimated by the supersonic airflow at the entrance of the combustor (**Eq. 6**).

Expansion wave

Figure 4 shows the expansion and confined waves. Considering no boundary-layer effects (non-viscous flow) and calorically perfect gas ($p = \rho RT$, $\gamma = \text{constant}$), the closed-forms of the thermodynamic property (static pressure, static density and static temperature) ratios across the expansion wave, which is limited by the head and tail of the expansion wave defined by the Mach angle μ_{head} , μ_{tail} , respectively, are given by (**Anderson, 1990**):

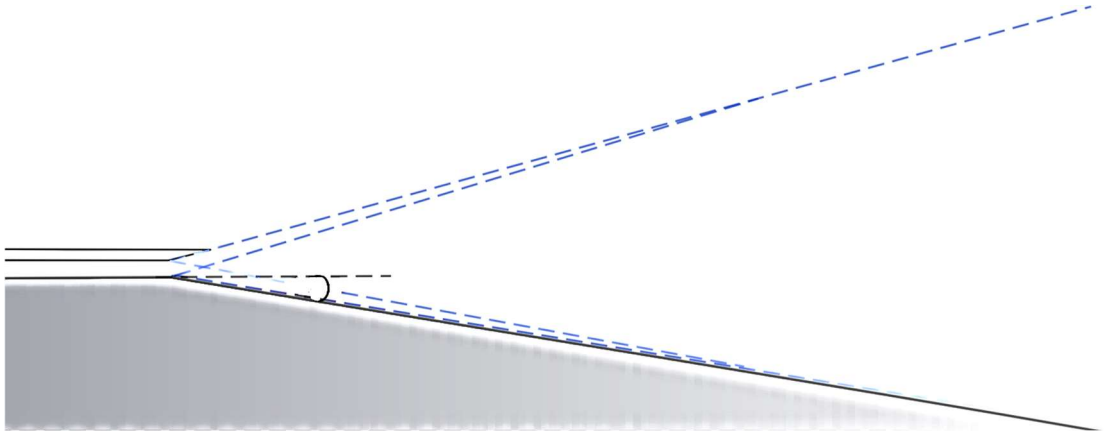

Figure 4: Expansion wave and confined expansion wave

$$\mu_{head} = \text{arcsen}\left(\frac{1}{M_{in}}\right) \tag{14}$$

$$\mu_{tail} = \text{arcsen}\left(\frac{1}{M_{out}}\right) \tag{15}$$

The expansion deflection angle θ_e is given by the Prandtl-Meyer function $\upsilon(\mathrm{M})$:

$$\theta_e = \upsilon\left(M_{out}\right) - \upsilon\left(M_{in}\right) \tag{16}$$

where the Prandtl-Meyer function $\upsilon(\mathrm{M})$ is given by:

$$\upsilon(M) = \sqrt{\frac{\gamma+1}{\gamma-1}}\ tg^{-1}\sqrt{\frac{\gamma-1}{\gamma+1}\left[M^2-1\right]} - tg^{-1}\sqrt{M^2-1} \tag{17}$$

Once Mach number after expansion wave M_{out} is determined by the closed form of the thermodynamic property (static pressure, static density and static temperature), the expansion wave may be obtained by the isentropic relationships given by:

$$\frac{T_{out}}{T_{in}} = \left(\frac{1 + \frac{\gamma - 1}{2} M_{in}^2}{1 + \frac{\gamma - 1}{2} M_{out}^2} \right) \tag{18}$$

$$\frac{p_{out}}{p_{in}} = \left(\frac{T_{out}}{T_{in}} \right)^{\frac{\gamma}{\gamma - 1}} \tag{19}$$

$$\frac{\rho_{out}}{\rho_{in}} = \frac{\frac{p_{out}}{p_{in}}}{\frac{T_{out}}{T_{in}}} = \left(\frac{T_{out}}{T_{in}} \right)^{\frac{1}{\gamma - 1}} \tag{20}$$

Note the flow across the expansion wave promotes a decrease of static pressure, static density, static temperature, and an increase of Mach number. The flow remains supersonic and parallel to the flat surface of the internal and external expansion section (**Fig. 4**) of the vehicle with airframe-integrated scramjet engine lower surface.

Area ratio (expansion wave)

If the supersonic flow that establishes the expansion wave is confined (**Fig. 4**), the head Mach wave strikes the lower surface of this confined environment and is reflected toward the upper surface. In this case, the Prandtl-Meyer theory is not valid anymore, and the area ratio should be applied (**Heiser and Pratt, 1994**). The reflected head Mach wave is assumed to be the same as the incident head Mach wave, which is given by

$$\frac{A_{out}}{A_{in}} = \frac{M_{in}}{M_{out}} \left(\frac{1 + \frac{\gamma - 1}{2} M_{out}^2}{1 + \frac{\gamma - 1}{2} M_{in}^2} \right)^{\frac{\gamma + 1}{2(\gamma - 1)}} \tag{21}$$

According to **Anderson (1990)**, it can be considered that the total temperature equation is obtained by interpolating **Equation 7** with the principle that $T_{total} = T_{in} + T_{out}$, thus obtaining the following equation:

$$T_{total} = 1 + \frac{\gamma - 1}{2} M^2 \tag{22}$$

2.3 Properties of the air

First step, it is necessary to define the thermodynamic atmospheric properties of the air, presented in **Table 1**. The generic scramjet will perform atmospheric flight, at 20 km of geometric altitude and speed corresponding to Mach number 5.8.

Table 1. Thermodynamic atmospheric properties at 20 km altitude (U.S. Standard Atmosphere, 1976).

Z (m)	H (m)	T (K)	p (Pa)	ρ (kg/m³)	a (m/s)
20	19935,28	216,65	5531,04	0,08894	295,07

2.4 Generic scramjet model

Figure 5 shows the schematic of the scramjet vehicle considered in the present study, composed by three ramps at the compression section, leading edge angle of 7.25º, and two deflection angles of 8.6º and 10.3º, respectively.

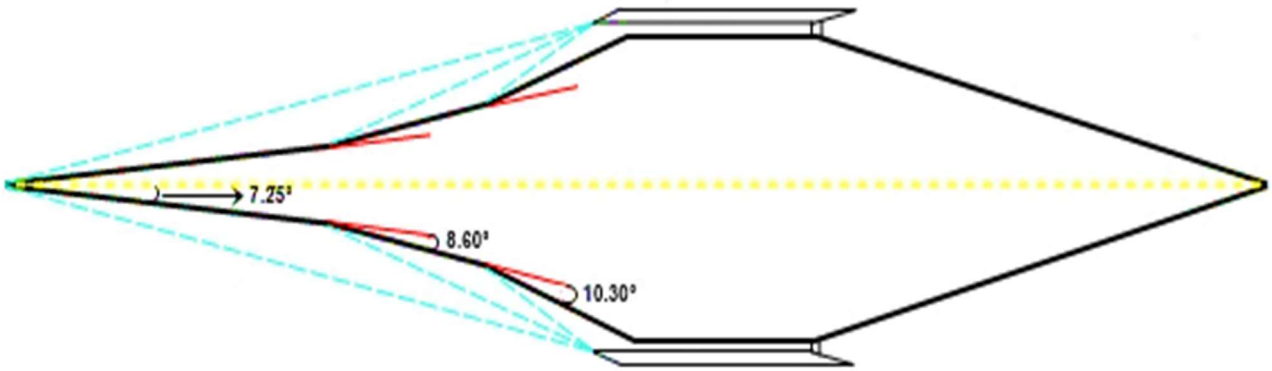

Figure 5. Cross section of the generic scramjet model

3. RESULTS AND COMMENTARIES

In **Table 2**, the relation β – θ – M (**Eq. 1**) is applied to obtain the incident oblique shock wave angles and the reflected oblique shockwave angles. Mach number after each incident and the reflected oblique shockwaves can be estimate by **equation 2**. Pressure, density and temperature can also be obtained at each stage, applying the **equations 3, 4** and **5**.

Table 2. Thermodynamic properties at the generic scramjet inlet, considering non-viscous flow, calorically perfect gas ($p = \rho RT$, $\gamma = 1.4$).

		Freestream	External compression surface (incident shock waves)			Internal compression Surface (Reflected shock wave)
			Ramp 7.25°	Ramp 8.6°	Ramp 10.3°	
M_{in}	-	5.80	5.80	4.87	4.04	3.29
θ_{in}	º	-	7.25	8.60	10.30	26.15
β_{out}	º	-	15.37	18.40	22.35	43.45
M_{out}	-	-	4.87	4.04	3.29	1.81
p_{out}	Pa	5531.04	14334.30	37135.68	96228.68	561058.25
ρ_{out}	kg/m^3	0.0889	0.1713	0.3299	0.6355	1.9328
T_{out}	K	216.65	291.48	392.11	527.53	1011.24
a_{out}	m/s	295.07	342.25	396.96	460.43	637.49
u_{out}	m/s	1711,40	1666.89	1605.09	1517.96	1154.23
T_{total}	K	1674.27	1674.27	1674.27	1674.27	1674.27

It is observed that the Mach number decreases at the compression section, but the pressure, density and temperature gradually increase. At the entrance of the combustion chamber the temperature and Mach number are 1011 K and 1.811, respectively, enough to burn spontaneously hydrogen at supersonic velocity.

Burning hydrogen at the combustion chamber, the Mach number of 1.1 was adopted for the air/hydrogen mixture (**Tables 3 and 4**).

Table 3. Thermodynamic properties at the combustion chamber and at the expansion section (with 10º), considering non-viscous flow and calorically perfect gas ($p = \rho RT$, $\gamma = 1.4$).

		Freestream	Combustor entrance (Tab. 2)	Combustor exit	$\theta_{Expansion} = 10^{o}$	
					Expansion section (Prandtl-Meyer)	Expansion section (area ratio)
M	-	5.80	1.81	1.10	1.48	5.35
P	Pa	5531.04	561058.25	1164090.67	696243.70	5259.22
ρ	kg/m^3	0.0889	1.933	2.524	1.7483	0.0533
T	K	216.65	1011.24	1606.79	1387.33	343.51
a	m/s	295.07	637.49	803.57	746.68	371,54
u	m/s	1711.40	1154.23	883.93	1105.57	1988.48
T_{total}	K	1674.27	1674.27	1995.63	1995.63	2311.32

Table 4. Thermodynamic properties at the combustion chamber and at the expansion section (with 15º) of the generic scramjet, considering non-viscous flow, calorically perfect gas ($p = \rho RT$, $\gamma = 1.4$).

		Freestream	Combustor entrance (Tab. 2)	Combustor exit	$\theta_{Expansion} = 15^{o}$	
					Expansion section (Prandtl-Meyer)	Expansion section (area ratio)
M	-	5.80	1.81	1.10	1.65	5.48
P	Pa	5531.04	561058.25	1164090.67	542864.93	5792.65
ρ	kg/m^3	0.0889	1.933	2.524	1.4636	0.0571
T	K	216.65	1011.24	1606.79	1292.12	353.12
a	m/s	295.07	637.49	803.57	720,60	376.71
u	m/s	1711.40	1154.23	883.93	1188.95	2068.07
T_{total}	K	1674.27	1674.27	1995.63	1995.63	2481.63

It was observed that pressure, temperature and density increased and Mach number descreased due to the heat addition, used to simulate the burning of hydrogen with air in supersonic combustion. However, temperature, pressure and density descreased and Mach number increased at expansion section.

The supersonic airflow at the entrance of the combustion chamber was the same for burning hidrogen/air at the combustion chamber. The combustion products conditions at the exit of combustion chamber were the same for both cases of 10º and 15º of deflexion angles at the expansion section, where the expansion Prandtl-Meyer and area ratios theories were applied. For both cases, Mach numbers at the scramjet trailing-edge were lower than the Mach number at the scramjet leading-edge. However, for both cases, the flow velocities at the scramjet trailing-edge were higher than the Mach number at the scramjet leading-edge. Therefore, in both cases, thrust was produced. Higher expansion deflection angle (15º) produced higher scramjet trailing-edge velocity, but longer expansion length.

4. CONCLUSION AND OUTLOOK FOR FUTURE PROJECTS

A generic scramjet vehicle, designed to fly at a geometric altitude of 20 km and at Mach number 5.8, applying the 1-D theoretical analysis, considering non viscous flow and calorically perfect gas was analyzed using the theory of shockwave theory, flow with heat addition on 1-D flow, and the theory of expansion wave (Prandtl-Meyer) theory coupled the area ratio are applied.

The data values of the variables considerate in the present work had variations, mostly for more. In the future, this model will be improved, tested in CFD (computational fluid dynamics) and will aim to be a hypersonic vehicle that transits freely at geometric altitudes of 20 to 30 km, obtaining the Mach number 5.8 reaching 10.

5. ACKNOWLEDGEMENTS

This study was financed in part by the Coordenação de Aperfeiçoamento de Pessoal de Nível Superior - Brasil (CAPES) – Finance Code 001. The three-first authors would like to thanks to Graduate Program in Aerospace Enginnering, at Universidade Federal do Rio Grande do Norte (UFRN, Natal/RN, Brasil) for financial support this project. This work has been partially sponsored by Universidade Federal do Vale do São Francisco (UNIVASF, Juazeiro/BA, Brasil) and the fourth author would like to extend his appreciation to support this project. Finally, the last author (as Visiting Professor) would like to express appreciation to UFRN the support given to complete this scientific work, also

the possibility to apply the knowledge in aerothermodynamics and hypersonics in the research area in hypersonic airbreathing propulsion based on supersonic combustion ramjet (scramjet) technology.

6. REFERENCES

Anderson, J. D., Modern Compressible Flow, The Historical Perspective. McGraw-Hill, Inc., ed. 2nd, 1990.

Cardoso, R. L., Sousa, M. S., Toro, P.G.P., Porto, B. F., "Dimensional Design of the Brazilian 14-X S Hypersonic Aerospace Vehicle for Flight Experimentation", to be presented at the 22nd Brazilian Congress of Mechanical Engineering, November 3-7, 2013, Ribeirão Preto, SP, Brazil.

Coordinating Research Council, Inc. "Aviation Fuel Properties". CRC Report No. 530, September 1983.

Curran, E.T., 2001. "Scramjet Engines: The First Forty Years". AIAA Journal of Propulsion and Power, Vol. 17, n. 6, p. 1138-1148. Nov. - Dez. 2001.

Hank, J.M., Murphy, J.S. and Mutzman, R.C., 2008. "The X-51A Scramjet Engine Flight Demonstration Program". In: 15th AIAA International Space Planes and Hypersonic Systems and Technologies Conference (AIAA 2008-2540), Dayton, Ohio, EUA.

Hass, N.; Smart, M.; Paull, A. "Flight Data Analysis of the HYSHOT 2". AIAA/CIRA 13th International Space Planes and Hypersonics Systems and Technologies Conference. Capua, Italy. 2005.

Heiser, W. H.; Pratt, D. T. Hypersonic Airbreathing Propulsion. Washington, D.C, American Institute of Aeronautics and Astronautics, 1994.

Marshall, L.A., Corpening, G.P. and Sherrill, R. A., 2005. "Chief Engineer's View of the NASA X-43A Scramjet Flight Test". In: AIAA/CIRA 13th International Space Planes and Hypersonic Systems and Technologies Conference (AIAA 2005-3332), Capua, Italia.

Moses, P. L.; Rausch, V. L; Nguyen, L. T.; Hill, J. R. "NASA hypersonic flight demonstrators – overview, status, and future plans". ACTA Astronautica, v. 55, p.619-630, 2004.

Pivetta, A. F. S., Camillo, G. P., Follador, R. C., Passaro, A., Rego, I. S., Minucci, M. A. S., Toro, P. G. P. "Design of an Academic unpowered axisymmetric scramjet for atmospheric captive flight at Mach number 4.18 using the Training Rocket FTI". CONEM 2016. Fortaleza, Brasil. 2016.

Rolim, T. C., Minucci, M. A. S., Toro, P. G. P. and Soviero, P. A. O., 2009, "Experimental Results of a Mach 10 Conical-Flow Derived Waverider". 16th AIAA/DLR/DGLR International Space Planes and Hypersonic Systems and Technologies Conference. AIAA 2009-7433. Santos, R. O., Minucci, M. A. S., Toro, P. G. P., Rego, I. S. "Concepção aerotermodinâmica e projeto mecânico de um motor scramjet de treinamento". CONEM 2016. Fortaleza, Brasil. 2016.

U.S. Standard Atmosphere. NASA TM-X 74335. National Oceanic and Atmospheric Administration, National Aeronautics and Space Administration and United States Air Force. 1976.

7. RESPONSIBILITY NOTICE

The authors are the only responsible for the printed material included in this scientific article.

The authors declare that there is no conflict of interest regarding the publication of this scientific article.